Energy Management of Distributed Generation Inverters in a Micro Grid by Using a Novel Control Strategy

A.Pravallika[1], G.SambasivaRao[2]

PG Student, Dept. of EEE, RVR&JC College of Engineering, Chowdavaram, Guntur, AP, India[1]

Associate Professor, Dept. of EEE, RVR&JC College of Engineering, Chowdavaram, Guntur, AP, India[2]

ABSTRACT: In This paper presents a small grid consisting of different distributed generation units those are connected to the distributed grid in this spatially A new energy management control technique implemented to coordinate the all Distributed generation units in the small grid. For grid connected and isolated operations. In this paper proposed a small grid consisting of PV and wind power systems FC and a storage battery, the design concept is verified through various test scenarios to demonstrate the operational capabilities of the proposed micro grid and verified in Matlab simulation software.

KEYWORDS: Distributed generation (DG),Wind, Pv, Energy management, micro grid model prediction control.

I.   INTRODUCTION

In the course of the most recent decade, proficient and solid correspondence what's more, control advancements, combined with an expansion in more quick witted electrical offices, for example, electric vehicles and brilliant meters, have brought about an expanding number of shoppers taking an interest demand response management (DRM) [1]–[5]. The ebb and flow look into is additionally centered around accomplishing a more quick witted grid through demand-side management (DSM), expanding vitality saves and enhancing the power nature of the conveyance system, for example, symphonies pay for nonlinear burdens [5]–[8]. These new patterns empower larger amounts of entrance of sustainable era, for example, wind and sun oriented power into the network. The coordination of sustainable sources can supplement the era from the conveyance system.

In any case, these inexhaustible sources are discontinuous in their era and might trade off the unwavering quality and soundness of the dissemination arrange. As In this project, a micro grid made up of a photo voltaic or (PV) range, proton-exchange membrane fuel cell (PEMFC), and a lithium-ion storage space battery (SB) is recommended. The PEMFC is utilized as a move down maker unit to compensate for the vitality created by the sporadic qualities of the PV range. The SB is executed for crest shaving amid lattice associated operation, what's more, to supply control for any lack in created control amid islanded operation and to keep up the strength of the appropriation arrange.

A vitality administration calculation is intended for the microgrid to arrange the sharing of energy among various DG units. In what takes after, this project gives a far reaching solution for the capacity of a micro grid which will in the meantime conveyance genuine and sensitive energy amid both network associated and islanded capacities, compensate for harmonics in the load voltages, and execute ideal cutting and burden losing under distinctive working circumstances.
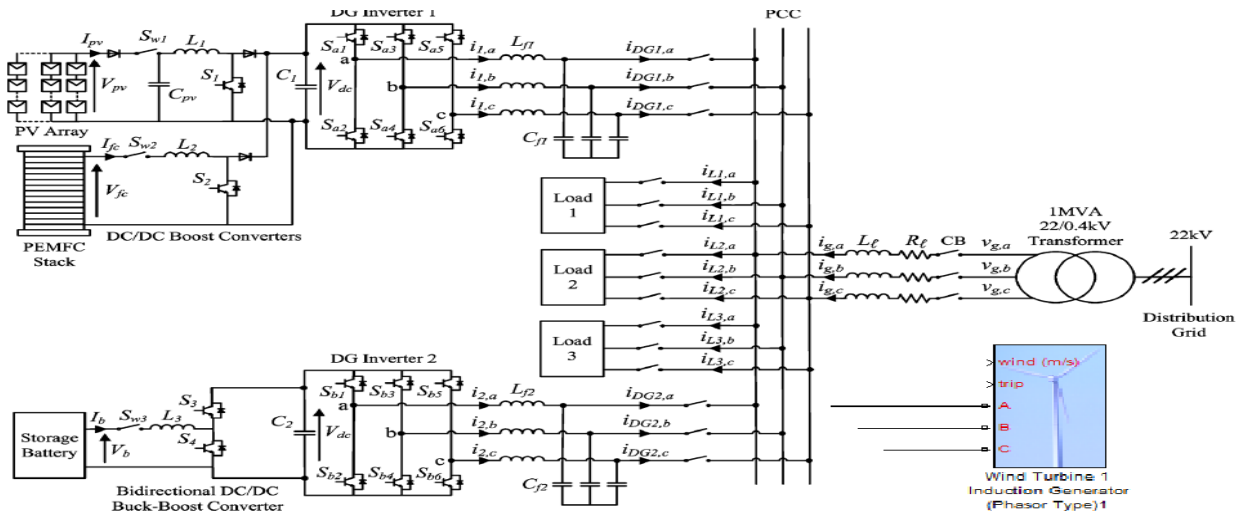
Fig. 1. Overall configuration of the proposed microgrid architecture.

A 40-kw photovoltaic array and a 15-kw prton exchange membrane fuel cell constitutes the the main DG unit in which the PV array act as the primary generation source and the PEMFC act as a secondary generation or backup generation but in the case of disconnection of PV array the PEMFC alone act as the main generation in order to given the required load.

Generally both the Wind PV array and the PEMFC are connected in parallel to the dc side of the DG inverter1 as shown in fig the proposed microgrid system design is such that it can be operated in both the modes that means either in grid connected or in islanded mode. The DC/DC boost converters regulate the output voltage of PV array and fuel cell stack and give the proper dc link voltage to the DG inverter1. When there is enough sunlight then the PV array operated in the MPPT mode to deliver the maximum dc power denoted by P_{pv} and the fuel cell generated power is denoted by $P_{fc.}$

The storage battery where considered is a lithium ion storage battery which is connected to the dc side of the 2nd DG inverter as shown in fig.5.1 the storage battery performs the charging and discharging operations according to the requirements. In the grid connected mode the SB aims for peak shaving and in the islanded mode it supplies some amount of power because of the absence of the distribution grid. During islanded operation the power delivered by SB and the main DG unit balances the total load given by the equation

$$P_{DG}+P_b=P_L \dots\dots\dots\dots\dots\dots\dots\dots\dots\dots\dots(1)$$

Under the constraint that

$$P_b \leq P_{b,max} \dots\dots\dots\dots\dots\dots\dots\dots\dots\dots\dots\dots(2)$$

By using the state of charge(SOC) the energy constraints are given by

$$SOC_{min} < SOC \leq SOC_{max} \dots\dots\dots\dots\dots\dots\dots(3)$$

Generally the SOC cannot be obtained directly but by using several estimation methods can easily determined. When the microgrid is islanded from the main grid the SB may be in the charging mode or discharging mode or idle mode that is purely depends on the state of charge and the power delivered by the storage battery. The state of charge must be in the limits of minimum to maximum SOC that means the value of the SOC should be less than or equal the maximum SOC and must be greater than the minimum SOC.

The power delivered by the SB must be satisfy the constraint that it should be less than or equal to the power delivered by the battery. The battery gets charging in the grid connected mode normally and discharging in the islanded mode it is also in the idle mode when there is power balance by the main DG unit and the distribution grid. The loads that are connected to the proposed system are of linear type and the nonlinear type also in the linear loads the load current does not contain any harmonics

but in nonlinear loads the currents get harmonics. In the grid connected mode the SB aims for peak shaving and in the islanded mode it supplies some amount of power. From the energy management system and its output the operation of the SB is summarized in the following fig under grid connected mode.
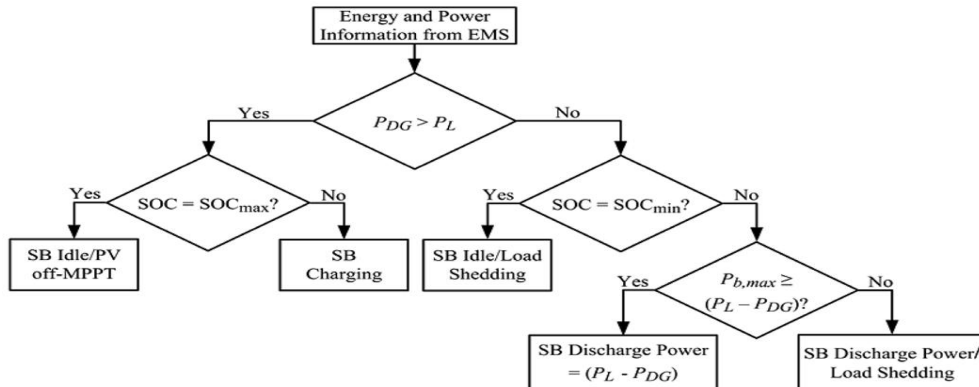

Figure 2 Operation of the SB during grid-connected operation

The output of the energy management system that is the power by main DG is more than the demand that cheks the SOC if it is maximum then the SB is in idle mode otherwise SB charge by the excess power. If the power by main DG is not more than the demand under such cases it verifies the off peak and peak periods in the off peak periods if the SOC is max SOC then the SB is in idle otherwise it is charged by grid. In peak periods if the SOC is equal to min SOC then the SB is in idle otherwise peak shaving.

During grid connected mode the main grid that is distributed grid is coupled with the micro grid at the point of common coupling(PCC). When a fault takes place in the main grid side then it is necessary to disconnect and it is performed by the CB and then the operation known as islanded operation. Then the main dg unit and the SB are the only main sources to meet the load under such conditions from the energy management system the operation of the SB are summarized. From the energy management system and its output the operation of the SB is summarized in the following fig under islanded mode.
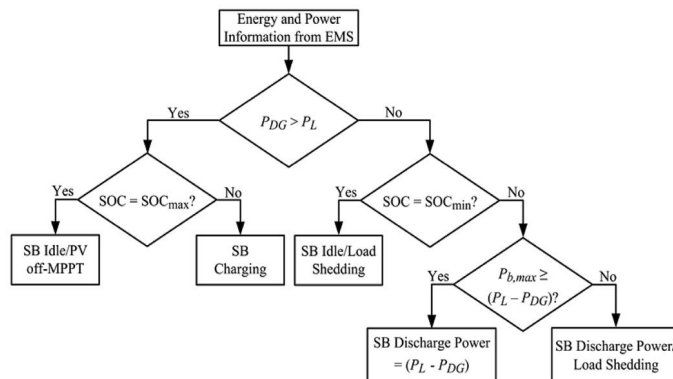

Figure 3 Operation of the SB during islanded operation

The output of the energy management system that is the power by main DG is more than the demand that cheks the SOC if it is maximum then the SB is in idle mode otherwise SB charge by the excess power. If the power by main DG is not more than the demand under such cases it verifies the SOC is min SOC then the SB is in idle otherwise

it cheks the condition that the maximum power delivered by the battery is more than the difference between the total load power to the main DG unit if it is yes then the SB discharges the power otherwise load shedding.

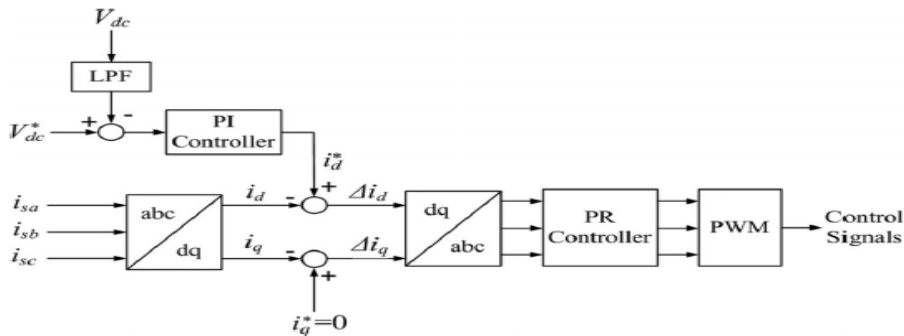### A CONTROL DESIGN FOR THE AC/DC CONVERTER

Fig 4 Configuration of the proposed controller for the ac/dc converter

Fig. above shows the configuration of the proposed controller for each ac/dc voltage source converter which is employed to maintain the dc output voltage V_{dc} of each converter and compensate for any variation in V_{dc} due to any power imbalance in the dc grid. The power imbalance will induce a voltage error ($V*_{dc} - V_{dc}$) at the dc grid, which is then fed into a proportional integral controller to generate a current reference $i*_d$ for i_d to track. To eliminate the presence of high frequency switching ripples at the dc grid, V_{dc} is first passed through a first-order LPF. The current i_q is controlled to be zero so that the PMSG only delivers real power. The current errors Δi_d and Δi_q are then converted into the *abc* frame and fed into a proportional resonant (PR) controller to generate the required control signals using pulse-width modulation.

B. DG INVERTER MODELING

The DG inverter modeling is a mathematical model. For the grid connected condition the equivalent single phase representation is shown in fig.4 For the islanded condition the equivalent single phase representation of the DG inverter
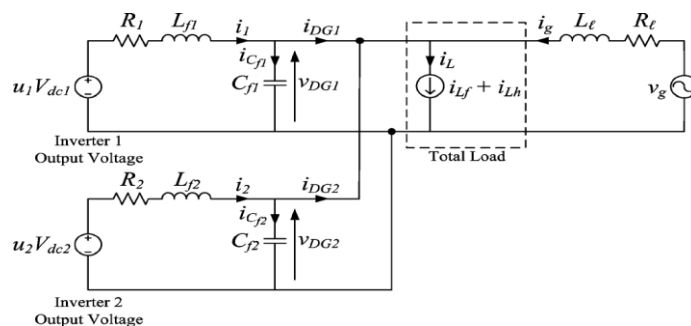

Figure 5 Equivalent single-phase representation of the DG inverters for grid connected operation

The output voltage across the inverter 1 is $u_1 V_{dc1}$ and across inverter 2 is $u_2 V_{dc2}$ where the u1 and u2 are the control inputs there are filters known as L, C filters which are represented by L_{f1} and L_{f2} and the C filters are given by C_{f1} and C_{f2}. These are the filters plays a important role to eliminate the harmonics from the voltage that is the output voltage of the inverter. The resistances R1 and R2 represent the loss of DG inverters. i_L represents the load current which is given by the equation

$$i_L = i_{L1} + i_{L2} + i_{L3} \quad \dots\dots\dots\dots\dots\dots\dots\dots\dots\dots\dots\dots\dots(4)$$

where the total load current is the sum of the indidual load currents, the first load in the proposed microgrid system is the non linear load and the second load is the linear load and the third load is also a nonlinear load the second load is a three phase RL load and the third load is a dimmer load.

The total load current can be written as two components consisting of two currents namely fundamental and harmonic currents represented by

$$I_L = i_{Lf} + i_{Lh} = I_{Lf} \sin(\omega t - \varphi_{Lf}) + \sum_{h=3,5,\dots}^N I_{Lh} \sin(h\omega t - \varphi_{Lh}) ..(5)$$

$$= I_{Lf} \sin\omega t \cos\varphi_{Lf} - I_{Lf} \cos\omega t \sin\varphi_{Lf} + \sum_{h=3,5,\dots}^N I_{Lh} \sin(h\omega t - \varphi_{Lh}) \dots(6)$$

$$= i_{Lf,p} + i_{Lf,q} + i_{Lh} \dots\dots\dots\dots\dots..(7)$$

The phase angles of fundamental current and harmonic current are involved in the load current equation
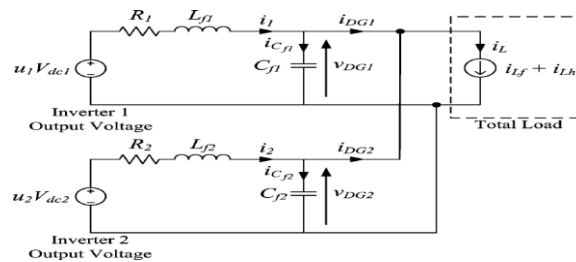

Figure 6 Equivalent single-phase representation of the DG inverters for islanded operation

It is required to get the unity power factor at the grid side by compensating the harmonics in the load currents for this purpose the DG unit deliveres a current which is denoted by i_{DGj} and is given by the equation

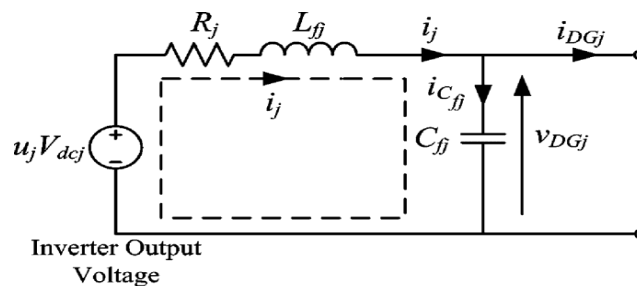$$i_{DGj} = (i_{Lf,p} - i_g) + i_{Lf,q} = i_{Lh} \dots\dots\dots(8)$$

Figure 7 Single phase representation of the jth DG inverter for grid connected and islanded operations

The grid current is i_g, from the fig.6 the v_g is the distribution grid voltage that acts as voltage source of the distribution grid, and from the fig.6 the R_l, L_l are resistance and inductance of the distribution line which acts as a link between the distribution grid voltage source and microgrid, loads.

The power dispatched to the load is controlled by controlling the output current of the DG inverter. In the grid connected operation it is done by current control mode(CCM) and in islanded operation entire microgrid is responsible therefore it is done by voltage control mode(VCM).

The state variable model under both conditions is obtained through the Kirchhoff's laws for the loop presented in the fig 6 that is for i_j loop then the equations are

$$\frac{di_j}{dt} = -\frac{R_i}{L_{fj}} i_j - \frac{1}{L_{fj}} \vartheta_{DGj} + \frac{V_{dcj}}{L_{fj}} u_j \dots\dots\dots\dots\dots (9)$$

$$\frac{dv_{DGj}}{dt} = \frac{1}{C_{fj}} i_j - \frac{1}{C_{fj}} i_{DGj} \dots\dots\dots\dots \dots\dots.(10)$$

The grid connected DG inverter state variable model is

$$x_{gj} = A_{gj}x_{gj} + B_{gj1}v'_j + B_{gj2}u_j \ldots\ldots\ldots\ldots\ldots\ldots\ldots (11)$$

$$y_{gj} = C_{gj}x_{gj} + D_{gj1}v'_j + D_{gj2}u_j \ldots\ldots\ldots\ldots\ldots.(12)$$

Where

$$A_{gj} = -\frac{R_j}{L_{fj}} ; B_{gj2} = \begin{bmatrix} -\frac{1}{L_{fj}} & 0 \end{bmatrix} ; B_{gj2} = \frac{V_{dcj}}{L_{fj}} : C_{gj} = 1 D_{gj1} = \begin{bmatrix} 0 & -C_{fj} \end{bmatrix} ; D_{gj2} = 0$$

$x_{gj} = i_j$ is the state : $v'_j = \begin{bmatrix} v_{DGj} & dv_{DGj}/dt \end{bmatrix}^T$ is the exogenous input; u_j is the control input, with -1≤u_j≤1;

and $y_{gj} = i_{DGj}$ is the output.

During islanded operation by following eq.(5.9) and (5.10) the state variable model is

$$x_{ij} = A_{ij}x_{ij} + B_{ij1}v'_j + B_{ij2}u_j \ldots\ldots..(13)$$

$$y_{ij} = C_{ij}x_{ij} + D_{ij1}v'_j + D_{ij2}u_j \ldots\ldots.(14)$$

Where

$$A_{ij} = \begin{bmatrix} -\frac{R_j}{L_{fj}} & -\frac{1}{L_{fj}} \\ \frac{1}{c'_f} & 0 \end{bmatrix} ; B_{ij1} = \begin{bmatrix} 0 \\ \frac{1}{c'_f} \end{bmatrix} ; B_{ij2} = \begin{bmatrix} \frac{V_{dcj}}{L_{fj}} \\ 0 \end{bmatrix} ; C_{ij} = \begin{bmatrix} 0 & 1 \\ 1 & -\frac{c_{ij}}{c'_f} & 0 \end{bmatrix}$$

$$D_{ij1} = \begin{bmatrix} 0 \\ \frac{c_{ij}}{c'_f} \end{bmatrix} ; D_{ij2} = \begin{bmatrix} 0 \\ 0 \end{bmatrix}$$

with $C'_f = \sum_{j=1}^2 C_{fj};$ $x_{ij} = [i_j \quad v_{DGj}]^T$ is the state vector;

$i'_j = i_L - \sum_{n\neq j} i_n$ is the exogenous input of the DG inverter ; is the control input, with ; and $y_{ij} = [v_{DGj} \quad i_{DGj}]^T$ is the

output.

II.   MODEL PREDICTIVE CONTROL DESIGN

The proposed microgrid system is a complicated system to provide the necessary control in this the new novel model predictive control MPC is used.

Model predictive control (MPC) is an superior method of process control that has been in use in the process industries in chemical plants and oil refineries since the 1980s. In recent years it has also been used in power system balancing models. Model predictive controllers rely on dynamic models of the process, most often linear empirical models obtained by system identification. The main advantage of MPC is the fact that it allows the current timeslot to be optimized, while keeping future timeslots in account. This is achieved by optimizing a finite time-horizon, but only implementing the current timeslot. MPC has the ability to anticipate future events and can take control actions accordingly. PID and LQR controllers do not have this predictive ability. MPC is a digital control.

The models used in MPC are generally intended to represent the behavior of complex dynamical systems. The additional complexity of the MPC control algorithm is not generally needed to provide adequate control of simple systems, which are often controlled well by generic PID controllers. Common dynamic characteristics that are difficult for PID controllers include large time delays and high-order dynamics.

MPC models predict the change in the dependent variables of the modeled system that will be caused by changes in the independent variables. In a chemical process, independent variables that can be adjusted by the controller are often either the set point of regulatory PID controllers (pressure, flow, temperature, etc.) or the final control element (valves, dampers, etc.). Independent variables that cannot be adjusted by the controller are used as

disturbances. Dependent variables in these processes are other measurements that represent either control objectives or process constraints.MPC uses the current plant measurements, the current dynamic state of the process, the MPC models, and the process variable targets and limits to calculate future changes in the dependent variables. These changes are calculated to hold the dependent variables close to target while honoring constraints on both independent and dependent variables. The MPC typically sends out only the first change in each independent variable to be implemented, and repeats the calculation when the next change is required.

While many real processes are not linear, they can often be considered to be approximately linear over a small operating range. Linear MPC approaches are used in the majority of applications with the feedback mechanism of the MPC compensating for prediction errors due to structural mismatch between the model and the process. In model predictive controllers that consist only of linear models, the superposition principle of linear algebra enables the effect of changes in multiple independent variables to be added together to predict the response of the dependent variables. This simplifies the control problem to a series of direct matrix algebra calculations that are fast and robust.

When linear models are not sufficiently accurate to represent the real process nonlinearities, several approaches can be used. In some cases, the process variables can be transformed before and/or after the linear MPC model to reduce the nonlinearity. The process can be controlled with nonlinear MPC that uses a nonlinear model directly in the control application. The nonlinear model may be in the form of an empirical data fit (e.g. artificial neural networks) or a high-fidelity dynamic model based on fundamental mass and energy balances. The nonlinear model may be linearized to derive a Kalman filter or specify a model for linear MPC.

The MPC is well suited for the fast sampling systems like microgrid systems.the state variable model of inverter modeling after time discretization may get the form of

$$x^+ = Ax + B_1 w + B_2 u \ldots\ldots\ldots\ldots\ldots\ldots\ldots\ldots..(15)$$
$$y = Cx + D_1 w + D_2 u \ldots\ldots\ldots\ldots\ldots\ldots\ldots.(16)$$

there are time shift operator with sampling intervels are represented by plus symbol. w is known as a periodic signal also known as exogenous signal.

This exogenous signal jointly with the reference d and with the output y forms a new model to keep in desired track given by

$$\xi^+ = A_\xi \xi \ldots\ldots\ldots\ldots\ldots\ldots\ldots\ldots\ldots\ldots...(17)$$
$$w = C_w \xi \ldots\ldots\ldots\ldots\ldots\ldots\ldots\ldots\ldots\ldots...(18)$$
$$d = C_d \xi \ldots\ldots\ldots\ldots\ldots\ldots\ldots \ldots\ldots\ldots\ldots..(19)$$

This state model is known as the exogenous system.

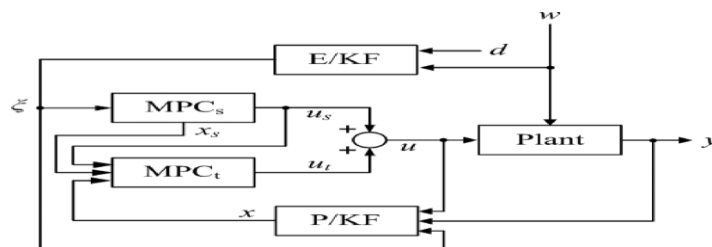The fig.23 represents the overall MPC controller with the kalman filter .

Figure 8 Overall MPC controller for the DG inverter with exogenous and plant kalman filter

Where the E/KF represents the exogenous kalman filter and P/KF represents the plant kalman filter.

The MPC controller optimizes the steady state as well as transient problem separately to reduce the computational complexity the steady state problem is defined as to satisfy

$$x_s{}^+ = Ax_s + B_1 w + B_2 u_s \ldots\ldots\ldots\ldots..\ldots\ldots.(20)$$

$$y_s = Cx_s + D_1w + D_2u_s \ldots\ldots\ldots\ldots\ldots\ldots(21)$$

Subject to

$$|u_s| \leq 1 \ldots\ldots\ldots\ldots\ldots\ldots\ldots\ldots\ldots\ldots(22)$$

And the transient problem is defined as to satisfy $x_t{}^+ = Ax_t + B_2u_t \ldots\ldots\ldots\ldots\ldots\ldots\ldots(23)$

$$y_t = Cx_t + D_2u_t \ldots\ldots\ldots\ldots(24)$$

Subject to

$$|u_s + u_t| \leq 1 \ldots\ldots\ldots\ldots\ldots\ldots\ldots(25)$$

And finally the the plant kalman filter is given by

$$x^{\sim+} = Ax^\sim + B_1w + B_2u + L_y(y - y^{\sim)}) \ldots\ldots(26)$$

$$y^\sim = Cx^\sim + D_1w + D_2u \ldots\ldots\ldots\ldots\ldots(27)$$

The loads are three the first load is a nonlinear load which is a three phase PWM adjustable speed drive its configuration is shown in fig.8
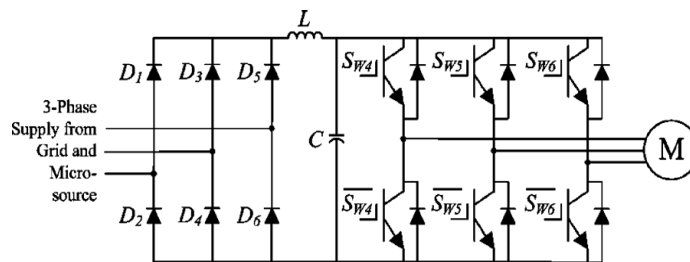
Figure 9 Configuration of a three phase ASD

It is a 15-kVA three phase adjustable speed drive there is a provision for the adjust. The source for this load is nothing but the three phase source from the grid and micro-system.
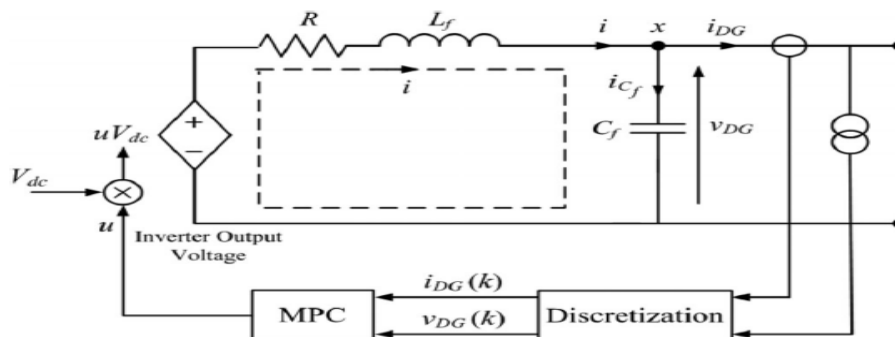

Fig 10 Single-phase representation of the three-phase dc/ac inverter.

To derive a state-space model for the inverter, Kirchhoff's voltage and current laws are applied to loop *i* and point *x* respectively, and the following equations are obtained:

$$Lf\, di/dt + iR + v\mathrm{DG} = uV\mathrm{dc} \quad (10)$$

$$iDG = i − iCf \ (11)$$

where Vdc is the dc grid voltage, u is the control signal, R is the inverter loss, Lf and Cf are the inductance and capacitance of the low-pass (LPF) filter respectively, iDG is the inverter output current, i is the current flowing through Lf, iCf is the current flowing through Cf, and vDG is the inverter output voltage.
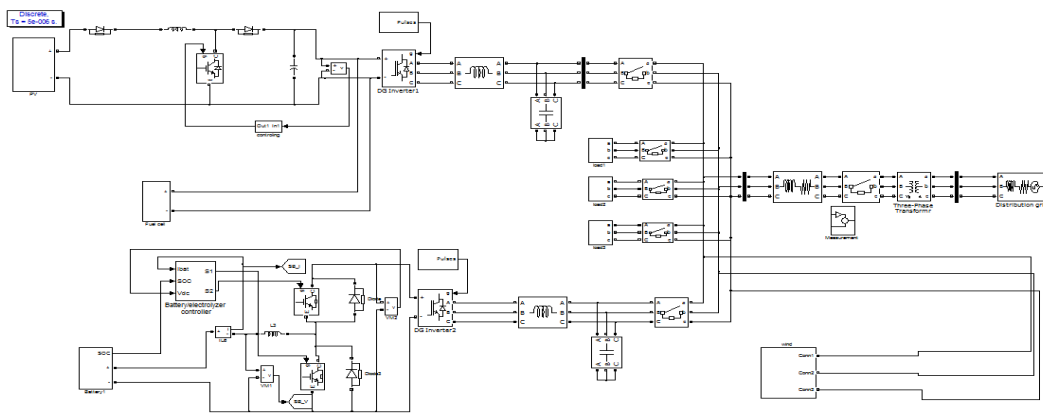
III. SIMULATION RESULTS

Figure 11 Simulink model for the proposed microgrid system

The simulink model consisting of the blocks of PV array, fuel cell and the storage battery which are the main renewable energy resources in the proposed system.the microgrid is tested under various conditions to evaluate its capabilities when operating connected and islanded from the distribution grid. Three different load types consisting of linear and nonlinear loads are considered in the studies.the parameters of the system are distribution grid voltage v_g=230V(phase),DC link voltage v_{dc}=400V,distribution line impedance R_l=0.0075Ω, L_l=25.7µH, LC filter L_f=1.2mH,C_f=20µF and DG inverter loss resistance R_f=0.01Ω. Load1 is a 15-kVA three phase PWM adjustable speed drive and load 2 is a RL load rated at active power of 28kW and reactive power of 18.5 kVAr. Load 3 is a three phase dimmer load rated at active power of 18kW and reactive power of 12.3 kVAr,which is nonlinear in nature.
The per phase currents drawn by loads 1,2 and 3 for $0 \leq t < 0.4$ is shown in fig.10
Due to the nature of nonlinearity of the loads 1 and 3 the waveform is not pure sinusoidal but the linearity of load 2 the load current wave form is purely sinusoidal.
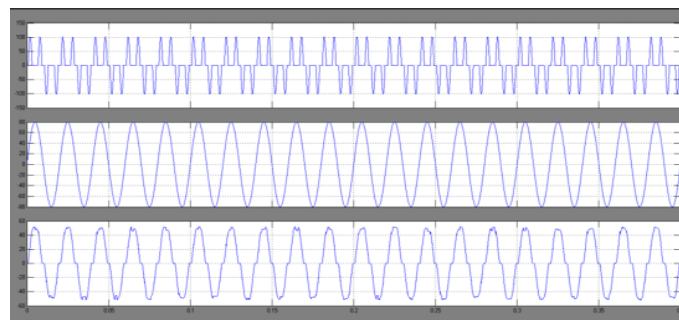

Fig 12 Per phase currents drawn by loads 1, 2,and 3.

A.Power quality improvement with load sharing during grid connected operation

Power quality improvement with load sharing during grid connected operatio demonstrates the capacity of the microgrod to improve the power quality of the distribution network by compensating the harmonics in the total load current due to the nonlinear loads that are connected to the distribution network, such that the harmonics will not propogate to the rest of the distribution network during grid connected operation.
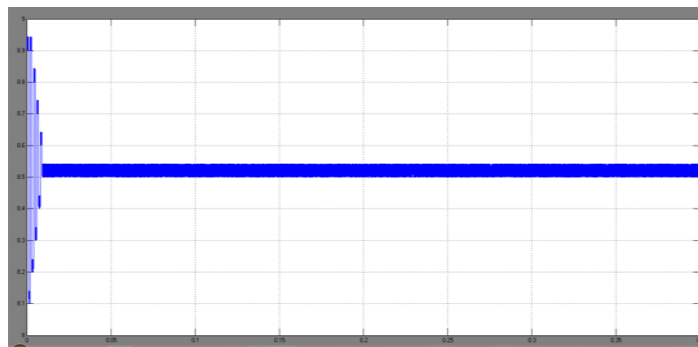The SB current for $0 \le t < 0.4$ are shown in fig.13

Fig 13 Waveform of the SB current during charging

The SB is operating in the charging mode to store energy during off-peak period where the cost of generation from the grid is low to meet future sudden demands for power.
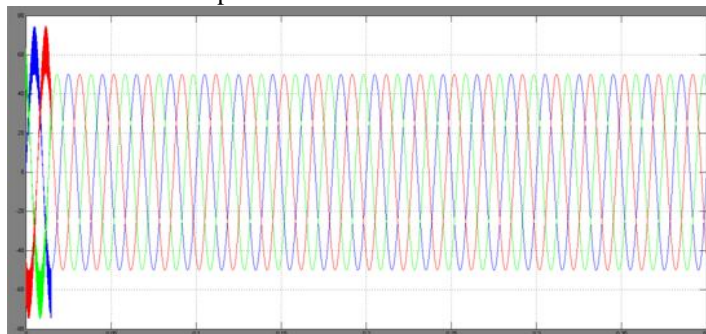

Fig 14 Waveform of three phase grid current

The waveforms of three phase DG current and three phase grid current the unsteady measurements are present for $0 \le t < 0.06$. are due to the fact that the controller needs a period of three cycles to track the generated references.
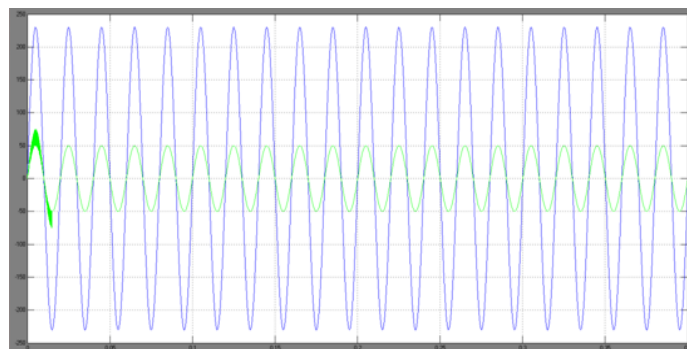

Fig 15 Waveforms of grid voltage and grid current for phase

The total real power and reactive power delivered to the loads is about 58kW and 35kVAr. The real power delivered to the load
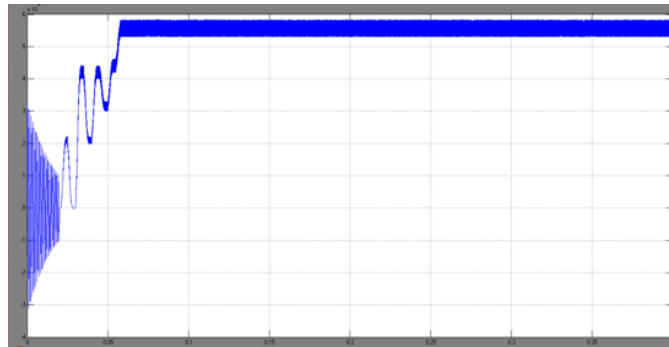

Fig 16 Real power consumed by loads

IV. CONCLUSION

In this paper coordinate The results have validated that the microgrid is able to handle different operating conditions effectively during grid-connected and islanded operations, thus increasing the overall reliability and stability of the micro grid.

REFERENCES

[1] S. Braithwait, "Behaviormanagement," IEEE Power and EnergyMag., vol. 8, no. 3, pp. 36–45, May/Jun. 2010.

[2] N. Jenkins, J. Ekanayake, and G. Strbac, Distributed Generation. London, U.K.: IET, 2009.

[3] M. Y. Zhai, "Transmission characteristics of low-voltage distribution networks in China under the smart grids environment," IEEE Trans. Power Del., vol. 26, no. 1, pp. 173–180, Jan. 2011.

[4] G. C. Heffner, C. A. Goldman, and M. M. Moezzi, "Innovative approaches to verifying demand response of water heater load control," IEEE Trans. Power Del., vol. 21, no. 1, pp. 1538–1551, Jan. 2006.

[5] R. Lasseter, J. Eto, B. Schenkman, J. Stevens, H. Vollkommer, D. Klapp, E. Linton, H. Hurtado, and J. Roy, "Certs microgrid laboratory test bed, and smart loads," IEEE Trans. Power Del., vol. 26, no. 1, pp. 325–332, Jan. 2011.

[6] A. Molderink, V. Bakker, M. G. C. Bosman, J. L. Hurink, and G. J. M. Smit, "Management and control of domestic smart grid technology," IEEE Trans. Smart Grid, vol. 1, no. 2, pp. 109–119, Sep. 2010.

[7] A. Mohsenian-Rad, V. W. S.Wong, J. Jatskevich, R. Schober, and A. Leon-Garcia, "Autonomous demand-side management based on gametheoretic energy consumption scheduling for the future smart grid," IEEE Trans. Smart Grid, vol. 1, no. 3, pp. 320–331, Dec. 2010.

[8] S. Chowdhury, S. P. Chowdhury, and P. Crossley, Microgrids and Active Distribution Networks. London, U.K.: IET, 2009.

[9] A. Yazdani and P. P. Dash, "A control methodology and characterization of dynamics for a photovoltaic (PV) system interfaced with a distribution network," IEEE Trans. Power Del., vol. 24, no. 3, pp. 1538–1551, Jul. 2009.